IEEE Access
Multidisciplinary | Rapid Review | Open Access Journal

IEEE POWER & ENERGY SOCIETY SECTION

Received January 14, 2021, accepted January 26, 2021, date of publication February 2, 2021, date of current version February 12, 2021.

Digital Object Identifier 10.1109/ACCESS.2021.3056454

An Energy Management System Design Using Fuzzy Logic Control: Smoothing the Grid Power Profile of a Residential Electro-Thermal Microgrid

DIEGO ARCOS-AVILES[1], (Member, IEEE), JULIO PASCUAL[2], (Member, IEEE), FRANCESC GUINJOAN[3], (Member, IEEE), LUIS MARROYO[2], (Member, IEEE), GABRIEL GARCÍA-GUTIÉRREZ[1], RODOLFO GORDILLO-ORQUERA[1], JACQUELINE LLANOS-PROAÑO[1], (Member, IEEE), PABLO SANCHIS[2], (Senior Member, IEEE), AND T. EMILIA MOTOASCA[4]

[1]Grupo de investigación en Propagación, Control Electrónico y Networking (PROCONET), Departamento de Eléctrica, Electrónica y Telecomunicaciones, Universidad de las Fuerzas Armadas ESPE, 171-5-231B Sangolquí, Ecuador
[2]Department of Electrical, Electronic and Communications Engineering, Public University of Navarre (UPNa), Edificio de los Pinos, Campus Arrosadia s/n, 31006 Pamplona, Spain
[3]Department of Electronics Engineering, Escuela Técnica Superior de Ingenieros de Telecomunicación de Barcelona, Universitat Politècnica de Catalunya, 08034 Barcelona, Spain
[4]VITO, BE-2400 Mol, Belgium

Corresponding author: Diego Arcos-Aviles (dgarcos@espe.edu.ec)

This work was supported in part by the projects 2019-PIC-003-CTE and 2020-EXT-007 from the Research Group of Propagation, Electronic Control, and Networking (PROCONET) of Universidad de las Fuerzas Armadas ESPE, in part by the Belgian Development Cooperation (DGD) and the VLIR-UOS under the project EC2020SIN322A101, in part by the Spanish Ministry of Industry and Competitiveness under Grant DPI2017-85404 and Grant PID2019-111443RB-100, and in part by the Spanish State Research Agency (AEI/10.13039/501100011033) under Grant PID2019-110816RB-C21 and Grant PID2019-111262RB-I00.

ABSTRACT This work deals with the design of a Fuzzy Logic Control (FLC) based Energy Management System (EMS) for smoothing the grid power profile of a grid-connected electro-thermal microgrid. The case study aims to design an Energy Management System (EMS) to reduce the impact on the grid power when renewable energy sources are incorporated to pre-existing grid-connected household appliances. The scenario considers a residential microgrid comprising photovoltaic and wind generators, flat-plate collectors, electric and thermal loads and electrical and thermal energy storage systems and assumes that neither renewable generation nor the electrical and thermal load demands are controllable. The EMS is built through two low-complexity FLC blocks of only 25 rules each. The first one is in charge of smoothing the power profile exchanged with the grid, whereas the second FLC block drives the power of the Electrical Water Heater (EWH). The EMS uses the forecast of the electrical and thermal power balance between generation and consumption to predict the microgrid behavior, for each 15-minute interval, over the next 12 hours. Simulations results, using real one-year measured data show that the proposed EMS design achieves 11.4% reduction of the maximum power absorbed from the grid and an outstanding reduction of the grid power profile ramp-rates when compared with other state-of-the-art studies.

INDEX TERMS Distributed power generation, energy management, power forecasting, fuzzy control, power smoothing, microgrid.

NOMENCLATURE

APD	Average Power Derivative
CMA	Central Moving Average
DG	Distributed Generation
DHW	Domestic Hot Water
DOD	Depth of Discharge
DR	Demand Response
DSM	Demand-Side Management
EMS	Energy Management System
ESS	Energy Storage System
EWH	Electric Water Heater

The associate editor coordinating the review of this manuscript and approving it for publication was Guangya Yang.

FLC	Fuzzy Logic Control
FPC	Flat-Plate Collector
HESS	Hybrid Energy Storage System
HRES	Hybrid Renewable Energy System
MF	Membership Function
MG	Microgrid
MILP	Mixed-Integer Linear Programming
MPD	Maximum Power Derivative
MPP	Maximum Power Point
PPV	Power Profile Variability
PV	Photovoltaic
RES	Renewable Energy Source
SMA	Simple Moving Average
SOC	State-Of-Charge
WT	Wind Turbine

I. INTRODUCTION

Distributed Generation (DG) systems have emerged as a great alternative to satisfy the growth of consumption demand, mitigate the effects of climate change and in turn contribute to the sustainable society development [1]. The use of DG systems, especially based on Renewable Energy Sources (RES), has significantly grown due mainly to environmental regulations, the shortage of fossil fuels, and the reduction of greenhouse gas emissions [2].

Several countries have promoted the use of DG systems mostly based on solar photovoltaic (PV) and wind turbine (WT) systems, in conjunction with energy storage systems (e.g., batteries, supercapacitors, fuel cells) [3], [4]. However, given the stochastic nature and high variability of both renewable resources and load demand, intelligent energy management systems are required that are capable of regulating the power flow among its elements and guarantee a reliable, safe, and economic operation of the system [5]–[7].

In this regard, microgrids (MG) [8], [9] arise as low power systems comprising DG elements, Energy Storage System (ESS), and an Energy Management System (EMS) which is in charge of controlling the power flow within the MG's elements to achieve a set of predefined objectives [10], [11]. Microgrids including renewable energies can be classified as smart-grids and can operate in both islanded and grid-connected modes. In stand-alone mode, where the MG is not connected to the distribution network, the EMS is in charge of keeping a reliable power supply to customers [12], [13], whereas in grid-connected mode, the MG adjusts the power balance between generation and demand by purchasing or selling power to the utility grid.

These systems have been in the focus of researchers for more than one decade, as confirmed by the abundant literature on this matter reported in recent review papers such as [14] and [15]. On the one hand, the large variety of microgrid EMS designs found in these works is at first due to the different energy scenarios under consideration (microgrid architectures, types, and controllability of DG sources, loads and storing technologies, . . .), as well as to the desired power fluxes among the MG elements and the grid to reach a set of goals. On the other hand, from a methodological point of view, the design of the EMS generally entails the definition of objective functions and optimization algorithms to reach the MG desired behavior by setting the power reference of MG controllable elements according to the available information (i.e., measured MG variables, weather conditions, and energy tariff forecasted data, . . .). In this respect, multiple possibilities have also been reported. For instance, referring to grid-connected microgrids, Table 1 mentions some research works to highlight the diversity of the cases in terms of scenarios, objectives, algorithms, and main controllable elements/available information, which can be found in the literature.

From Table 1, besides the different scenarios, it can be noticed that a large set of objective functions found in the literature are oriented to optimize the economical balance between cost and benefit of the microgrid operation along a given time period. This is directly related to the power exchange allowance between the grid and the MG facilitating the owner to become a prosumer and benefit from the tariff policies established by grid stakeholders. However, the feasibility of this approach is limited by the grid capability to manage power variations without instabilities [16]–[19]. That is why the definition of objective functions following these economical goals involves, among others, grid tariff policies and user comfort criteria, but rarely power quality indexes, being the grid and MG operational limits included as constraints in the algorithms in charge of the optimization process. Finally, it can be pointed out that the methods/algorithms driving the EMS strategy are generally on-line ones requiring different levels of computational load and communication facilities.

This work presents several differences with the antecedents cited in Table 1. On the one hand, it focuses on the design of an EMS when RES and storing capabilities are included in the supply of pre-existing grid-connected household appliances. The energy scenario considers a residential MG comprising PV and WT generators, flat-plate collectors (FPC), electric and thermal loads, and electrical and thermal ESSs. The operating conditions assume that the generators should operate at their maximum power point (MPP) to take the maximum profit of renewable generation, and both electric and thermal loads only driven by the user according to his comfort standards. This means that neither the renewable generation nor the loads are controllable. As concerns the available information, this scenario was implemented years ago in a physical residential grid-connected MG monitored with metering devices recording real data of renewable production and load consumption every 15 minutes. This monitoring allows the access to historical data recorded in one year. Additionally, forecast weather and consumption data are also considered available.

On the other hand, the main goal of the EMS is to smooth the power profile exchanged with the mains to reduce the impact on the grid power when RES are incorporated to supply pre-existing grid-connected household appliances. That

TABLE 1. Literature review.

Ref.	Scenario (MG elements)	EMS Objectives/Constraints	Methodology/algorithms	Main controlled Variables/Available information
[20]	Photovoltaic (PV), wind turbine (WT), genset, battery energy storage system (ESS), households Heating, Ventilation and Air Conditioning (HVAC), and electric water heater (EWH).	Minimize the total microgrid (MG) cost comfort priorities of individual households' preservation.	Stochastic mixed-integer linear programming (MILP) model with 24-hour rolling horizon.	HVAC system, EWH.
[21]	PV, battery ESS (Li-ion battery cell), and loads. MG power injection to the mains not allowed.	Optimize the operational electricity cost of the microgrid in the next 24h.	Nonlinear programing with discontinuous derivatives.	PV power, battery power, battery efficiency, battery state-of-charge (SOC), grid power.
[22]	Micro-turbine, WT, PV systems.	Coordinate the price-based demand response (DR) and dispatchable distributed generators (DG) for robust and optimal operation of the microgrid. Maximize the overall profit satisfying operational limits.	Two stages coordinate Price-Based DR and dispatchable DG.	WT power, PV power, Micro-turbine power, day-ahead market price, day-ahead load demand, day ahead WT and PV power.
[23]	Smart home equipped with ESS and dispatchable loads.	Scheduling process for power consumption to reduce electricity bills and improve the peak-to-average ratio while taking into account the comfort of the residents.	Multi-objective optimization problem solved with non-dominated sorting genetic algorithm using Matlab.	Appliances scheduling operating time (deferrable loads), battery SOC.
[24]	Residential MG with various types of distributed energy resources (DER) and intelligent household devices.	Reduce domestic energy usage while improving the user's satisfaction degree and comfort.	Two stage optimization problem. Demand-side management (DSM) algorithm.	Load scheduling, battery SOC, DER power, thermal energy, gas consumption, satisfaction degree.
[25]	Grid-connected PV inverters with battery storage.	Maximize the revenue over a given time period while meeting the battery stored energy constraint.	Lagrange multipliers. DR algorithm.	Forecast of PV output, average daily PV power output.
[26]	Industrial MG with eight thermal plants, two wind farms, three main aluminum electrolysis loads (controllable), two heat loads (uncontrollable), and four auxiliary loads (uncontrollable).	Smoothing the tie-line fluctuations between industrial MG and the utility grid using demand-side approach.	DSM algorithm, linear quadratic-based output, regulator theory.	WT power, WT Frequency, forecast power
[27]	Residential rooftop PV and battery ESS, controllable and uncontrollable loads.	Autonomous energy consumption scheduling algorithm to shift the operation of deferrable loads from peak consumption hours to hours with high-power generation from PV units.	Stochastic programming to formulate an energy consumption scheduling problem.	PV power, load power, loads schedule.
[28]	Low-voltage autonomous MG comprising five dispatchable DG units, three WT, two PV units, and loads.	Maximize the expected profit of the microgrid operator through optimal scheduling of resources considering both supply and demand side uncertainties.	Stochastic risk-constrained framework. Monte-Carlo simulation. DR algorithm.	Electricity price, RES power and uncertainties, load power and uncertainties, grid power, wind power forecast.
[29]	Building energy management with rooftop PV system, ESS, virtual ESS, controllable and uncontrollable loads.	Coordinate and manage the operation of all electrical loads and DER to determine optimal day-ahead energy quantity bids considering the expected cost of real-time imbalance trading under uncertainty	Optimization based on day-ahead scheduling and bidding. DR approach.	Load scheduling, real-time electricity price.
[30]	PV, WT, micro-turbine, home fuel cell (FC), battery ESS, electric vehicle (EV), and controllable loads.	Minimize the costs associated with consumption, the consumers comfort and environmental pollution. Determination of new operation periods for home appliances.	Constrained non-dominated sorting, genetic algorithms. DR approach.	Real-time electricity price, electricity consumption, ESS, PV, WT, and EV powers.
[31]	Micro-turbine, FC, battery bank, WT, PV.	Generation and a controllable load demand policies minimizing over a planning horizon the operation costs subject to economic and technical constraints.	MILP	PV, WT, and micro-turbine powers, ESS power, grid power.

TABLE 1. *(Continued.)* **Literature review.**

[32]	Different ESS (electricity and heat), combined heat and power (CHP) units, and different DER.	Optimal scheduling considering technical and economic ties between electricity and natural gas systems to reduce the operation cost of the system.	MILP	CHP power, day-ahead electricity price, gas price, load power, active power exchange between the MG and mains.
[33]	Multi-microgrid system comprising WT and PV generators, battery ESS, and loads.	Minimize the operating cost of the energy storage system unit and minimize the net value of unexpected power transactions with the main grid.	Hierarchical control structure. Stochastic optimization. Monte-Carlo simulation.	Grid power, battery SOC, renewable energy systems (RES) forecast data, load consumption, RES production.
[34]	Smart home with bidirectional metering and communication, utility grid, RES, ESS, EV, EWH, and domestic appliances.	Home energy management system to intelligently schedule the operation of domestic appliances, RES, ESS, EV for a minimum cost of electricity with guaranteed user satisfaction.	MILP	RES generation, consumption power, utility power, EWH power, electricity price, water temperature.

is why, instead of considering grid operational limits as constraints in the optimization process, the objective function considered in this work directly involves grid power quality indexes. In other words, this work prioritizes smoothing the power profile exchanged with the grid keeping the load demand according to the user needs and leaving economic benefits as a desirable consequence. Finally, as concerns the optimization algorithms, this work will optimize the objective function of designing low-complexity Fuzzy Logic Controllers (FLC) since they facilitate the implementation of the microgrid control policies through linguistic rules of easy understanding. These FLC will be adjusted through an off-line training procedure. To conclude, the rationale of the proposed approach is the design of a low-complexity EMS for a grid-connected residential microgrid with low control degrees of freedom, which mitigates the interaction with the mains. This is intended to facilitate the transition from a conventional electric supply to a progressive renewable-based one.

The authors worked during the last years in this scenario on the design an EMS to ''smooth'' the profile of the power exchanged between the microgrid and the grid by employing a set of quality indices to measure the degree of smoothness of such profile [35], [36]. Early works considered a simple grid-connected electrical microgrid, including an ESS, RES, and a residential electrical load [36], [37]. The MG operation assumed the ESS as the only controllable element since RES operated at their MPP to maximize RES production and the load consumption was not manageable. Under these assumptions, the main antecedents attempting to reduce peaks and fluctuations in the power profile exchanged with the grid can be found, for instance, in [38], [39]. In these works the EMS design is based on the use of a Simple Moving Average (SMA) filter (low-pass filter with a window size of 1 day) to split the microgrid power balance spectrum, so that only the low-frequency components are exchanged with the mains, whereas high-frequency ones were absorbed by the ESS. From the control point of view, these strategies were open-loop control strategies and did not take into account the state-of-charge (SOC) of the ESS whose capacity should be oversized to assure its operation within secure limits. A control strategy of the SOC was presented in [40] by defining a set of heuristically adjustable analytical expressions driving the power-sharing between the ESS and the mains. This work also included the SMA filter, but now acting on the resulting grid power-sharing. However, this strategy preserved the ESS operation at the expense of grid power high fluctuations. Due to its heuristic nature, this procedure was especially suitable to be improved by using expert knowledge rule-based systems based on FLC [41]. FLC have proven to be of easy implementation and low computational run time cost than other sophisticated analytical solutions such as those reported in [42], [43]. As a result, an FLC-based EMS of only 25 rules with an off-line FLC parameters tuning, using measured RES generation and load consumption data for one year, was suggested in [44] and [10]. This design was implemented, experimentally tested, and confirmed the better performances on the grid power profile smoothness than those given in [40], while preserving the ESS SOC operation within prefixed safe operation limits. However, a common drawback of the previous EMS designs is the use of the SMA filter with a window size of 24h, since it introduces a lag into the EMS response and leads to degraded features when weather conditions show a great difference from one day to the next one. This problem was solved in [36] by considering a 24h Central Moving Average (CMA) filter instead of the commonly used SMA filters. This strategy takes advantage of the 12h ahead forecast of generated and consumed power in the microgrid to obtain a better grid power profile with efficient usage of the ESS. Moreover, following the same methodology, a new FLC-based design improving the grid power profile of [36] was presented in [11]. A review of the complete design criteria of the FLC parameters for all the aforementioned cases can be found in [45].

On the other hand, the power profile smoothness can be further improved if the scenario includes a Domestic Hot Water (DHW) power consumption driven by a controllable

Electrical Water Heater (EWH). An interesting and successful approach can be found in [35], where the authors apply a demand-side management (DSM) technique to drive the EWH as a controllable load. The main idea of the design is to use the thermal storage capacity of the water tank to relieve the stress of the ESS and to improve the grid power profile. In this concern, the power share among the ESS, the EWH, and the mains is once again heuristically adjusted to concurrently improve the smoothness of the mains power while keeping both the water tank temperature and the ESS SOC within desired limits. However, this work still uses an SMA filter and does not take advantage of forecast data regarding generated and consumed power in the microgrid.

In order to better smooth the grid power profile, this paper proposes an EMS design for a grid-connected electro-thermal microgrid merging the advantages of using an FLC to better tune the heuristic approach of [35], combined with the use of forecasted power generation and consumption data (including the thermal one). Following the idea exposed in [35], but under an FLC perspective, this design uses the electrical and thermal power balance of the microgrid together with its predictions to perform the suitable DSM of the EWH controllable load. Simulation results using one year real data provided by the microgrid installed at the Public University of Navarre (UPNa) are compared with those obtained in [35] to highlight the improved features of the proposed design in terms of smoothing the power profile while keeping the ESS SOC and the temperature of the water tank within desired limits. Moreover, the design also includes the possibility to limit the peak value of the power injected into the mains.

The main contributions of this work are listed below:

1) An EMS control block-diagram based on two FLC blocks of only 25 rules each, to smooth the grid power profile of a residential grid-connected electro-thermal microgrid.
2) The complete design of each of the two FLC blocks using the electro-thermal power balance of the microgrid as well as the forecasted data of power generation and consumption. The first FLC block is in charge of smoothing the power profile exchanged with the grid, whereas the second FLC block is responsible for performing the DSM of the EWH.
3) A set of comparative one-year simulations and quantification of smoothing indexes using real data both highlights the improved performances of the proposed approach.

The remainder of this paper is organized as follows: Section II presents the electro-thermal microgrid architecture under study. Section III describes the criteria associated with the quality of the grid power profile. Section IV deals with the fuzzy-based EMS design. Section V presents the simulation and comparison results. Finally, Section VI presents the main conclusion of this work.

II. ELECTRO-THERMAL MICROGRID POWER ARCHITECTURE

The microgrid under study has been previously described in [35], [45]–[47] and it is shown in Fig. 1. The figure highlights the DHW system with FPC, EWH, the water tank, and the DHW consumption. Its elements and the power sizes (out of the scope of this work) are described below in short:

1) Hybrid electrical renewable energy system (HRES) including a 6kWp PV generator, a 6kW WT, and a 2kW FPC.

2) Hybrid Energy Storage System (HESS) consisting of a lead-acid battery bank with a usable capacity of 36kWh and an 800l capacity water tank.

3) Thermal and electrical loads with the equivalent thermal demand rated at 2kW. These loads are divided according to their controllability, into:

- Non controllable electrical AC loads (electrical appliances, lighting…) of 7kW.
- A EWH of 2kW rated power considered as a controllable load.

As described in [11], the INGECON® Hybrid Inverter shown in Fig. 1, includes a WT power conversion module, a battery charger and a PV power conversion module, together with a bidirectional inverter-rectifier module for controlling the grid power profile. It is worth noting that the battery charger has an internal active power control, whereas the bidirectional inverter-rectifier has both active and reactive power control. The EMS provides the reference values of the active power for battery charger and inverter rectifier and of the reactive power for the inverter. Since the reactive power does not have associated energy, the bidirectional inverter-rectifier can supply all reactive power of the load as long, as the apparent power does not exceed its nominal value [11]. Therefore, the EMS is responsible for measuring the load reactive power and delivering it, as the reference value, to the inverter-rectifier.

The following power balance expressions can be defined considering a positive power flow according to the direction of the arrows depicted in Fig. 1:

$$P_{BAL}(n) = P_{LOAD}(n) + P_{DHW}(n) - P_{PV}(n) - P_{WT}(n) - P_{SC}(n) \quad (1)$$

$$P_{BAT}(n) = P_{LG}(n) - P_{GRID}(n) + P_{EWH}(n) \quad (2)$$

$$P_{LG}(n) = P_{LOAD}(n) - P_{PV}(n) - P_{WT}(n) \quad (3)$$

where P_{BAL} is the MG's overall power balance, P_{LOAD} is the residential power demand, P_{DHW} is the equivalent of domestic hot water power consumption, P_{PV} and P_{WT} are the rated photovoltaic and wind turbine powers, respectively, P_{SC} is the FPC thermal power, P_{BAT} is the battery power (i.e., $P_{BAT} > 0$ for discharging process and $P_{BAT} < 0$ for charging process), P_{LG} is the MG electrical net power, P_{GRID} is the power exchanged with the mains (i.e., $P_{GRID} > 0$ for injection to the MG and $P_{GRID} < 0$ for absorption from the MG), and P_{EWH} is the power required by the EWH.

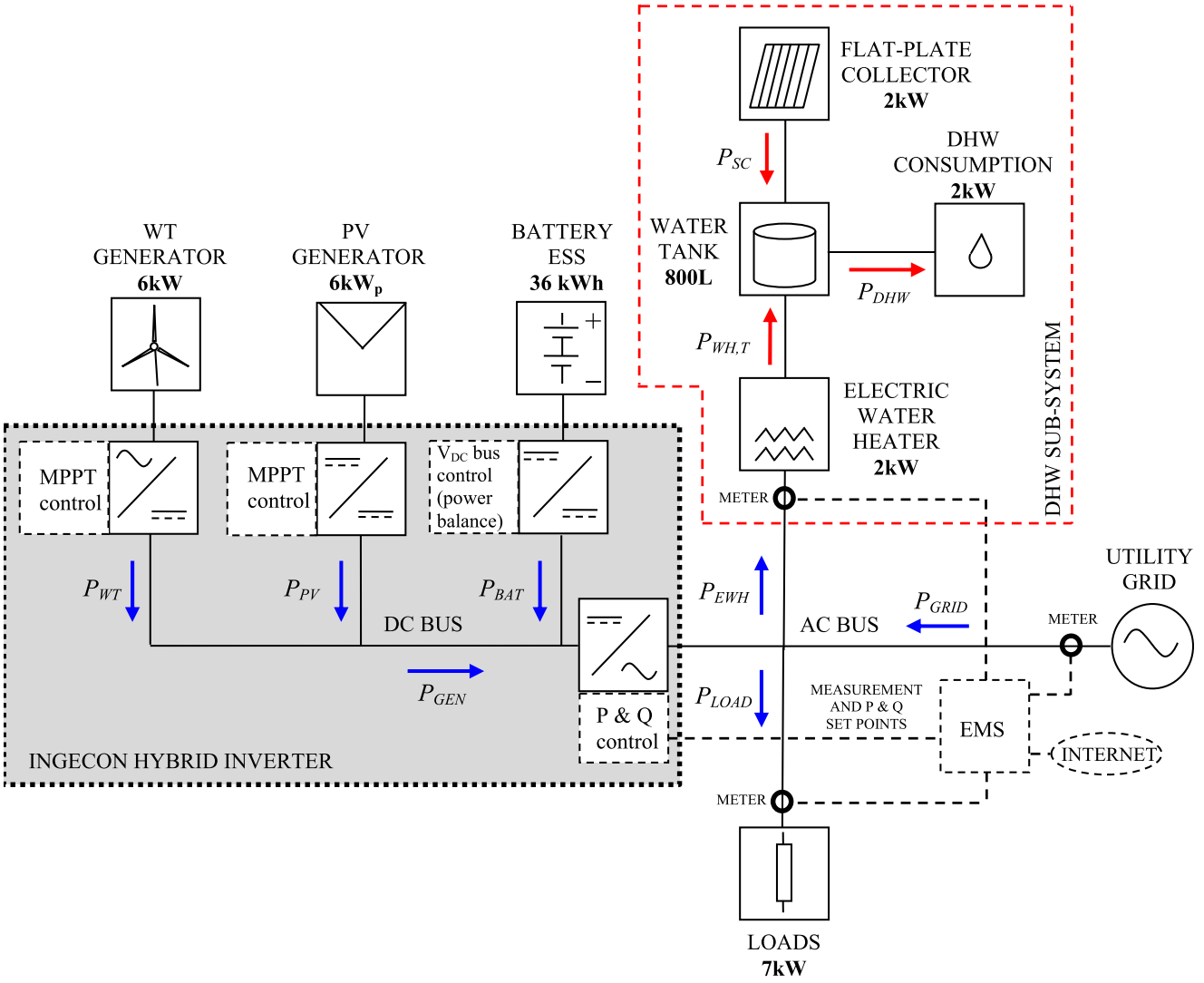

FIGURE 1. Residential grid-connected electro-thermal microgrid architecture.

Note that the case under study assumes that both PV and WT are operating at their MPP and both thermal and electrical load consumptions are given. Therefore, neither the renewable power generation nor the consumptions are controllable. In contrast, the DHW system includes a controllable load, i.e., electric water heater. In short, the grid profile will be controlled by the bidirectional inverter-rectifier as long as the battery charger can handle the resulting battery power P_{BAT}. In this regard, the battery power directly depends on the current battery SOC, which must be kept between secure limits to preserve ESS lifetime. Since this study considers a battery pack composed of lead-acid batteries, a maximum allowable Depth of Discharge (DOD) of 50% is imposed [48]. Therefore, the battery SOC boundaries are defined as follows:

$$SOC_{MIN} \leq SOC(n) \leq SOC_{MAX} \quad (4)$$

$$SOC_{MIN} = (1 - DOD) \cdot SOC_{MAX} \quad (5)$$

where SOC_{MIN} and SOC_{MAX} the minimum and maximum battery SOC limits, respectively, and $SOC\ (n)$ can be computed using the SOC estimator block presented in [10], [11], [45].

The thermal storage capacity associated with the water tank temperature, is responsible for improving the system performance by providing a thermal buffer to alleviate the solar availability or load mismatch [46], [49]. In this regard, the water tank and the controllable load (i.e., EWH) provide extra possibilities to control the grid power profile.

Therefore, suitable control of the water tank temperature is required to meet the user's consumption needs. In this context, the mathematical model (out of the scope of this work) to estimate the water temperature in the thermal storage must consider the physical characteristics of the tank and also the energy rates of the different variables involved in the water heating process. A complete description of the thermal storage model can be found in [45], [47]. Note that this study

considers that the water temperature should be kept in the range between 35°C and 75°C.

III. GRID POWER QUALITY CRITERIA

A set of quality criteria is defined in order to evaluate and compare different EMS designs to be described in the following paragraphs. The grid power profile quality criteria are defined to quantify the improvement of the power profile exchanged with the grid obtained by a specific energy management strategy. For instance, when concerning the power exchanged with the grid, an EMS is considered to have better performance when the values of the quality criteria are minimized. These quality criteria are based on the grid profile averaged every fifteen minutes (i.e., $T_s = 900$s) and have been defined in [10], [11], [35], [36], [45]. Here they are recalled in the following paragraphs for the sake of paper completeness.

A. POSITIVE AND NEGATIVE GRID POWER PEAKS

The positive grid power peak, $P_{G,MAX}$, is defined as the maximum power delivered by the mains in one year, whereas the negative grid power peak, $P_{G,MIN}$, is defined as the maximum power fed into the mains (i.e., maximum power injected by the MG to the mains) in one year. These criteria are computed as follows:

$$P_{G,MAX} = \max(P_{GRID}) \tag{6}$$

$$P_{G,MIN} = \min(P_{GRID}) \tag{7}$$

B. MAXIMUM POWER DERIVATIVE

The maximum power derivative (MPD) is defined as the maximum yearly value, in absolute value, of the grid power profile slopes, $\dot{P}_{GRID}$. This criterion is expressed in W/h and it is computed as follows:

$$MPD = \max\left(\left|\dot{P}_{GRID}\right|\right) \tag{8}$$

$$\dot{P}_{GRID}(n) = [P_{GRID}(n) - P_{GRID}(n-1)]/T_s \tag{9}$$

C. AVERAGE POWER DERIVATIVE

The average power derivative (APD) is computed as the annual average value of the absolute value of $\dot{P}_{GRID}$. Similarly to MPD criterion, APD is expressed in W/h:

$$APD = \frac{1}{N}\sum_{n=1}^{N}\left|\dot{P}_{GRID}(n)\right| \tag{10}$$

where N is the number of samples in a year.

D. POWER PROFILE VARIABILITY (PPV)

This criterion measures the grid power profile variability and is defined as:

$$PPV = \sqrt{\sum_{f=f_i}^{f_f}\left(P_{GRID,f}\right)^2}/P_{DC} \tag{11}$$

where $P_{GRID,f}$ is grid power harmonic at frequency f, f_i and f_f are the initial and final frequencies, respectively and, P_{DC} is the yearly power average value. This criterion only evaluates frequencies above $f_i = 1.65 \times 10^{-6}$ Hz (i.e., variation periods of one week or less), since the energy management strategy seeks to compensate daily variations. Furthermore, the maximum frequency considered to calculate PPV is half of the sampling frequency $f_f = 5.55 \times 10^{-4}$ Hz.

Note that variable renewable energy sources, such as PV and WT, are set to attain very high degrees of penetration level. Thus, the power variability is of great concern for grid operators [50]–[52]. In this regard, MPD and APD criteria represent power fluctuations in the grid and, hence they are related to grid instability.

IV. FUZZY ENERGY MANAGEMENT ARCHITECTURE

As shown in Fig.2, the proposed EMS is built out of three main blocks: (1) MG power balance; (2) thermal power balance and demand management; and, (3) a grid power injection limitation, which simply clamps the power at a desired upper limit value. These blocks are described below:

A. BLOCK 1: MG POWER BALANCE - BATTERY SOC CONTROL AND GRID POWER COMPONENTS

The first block in Fig.2 is in charge of computing the value for the grid power profile before the power clamper of Block 3. This grid power is noted as P_G^{S1} and the control strategy principle for its computation is very similar to that presented in [11] excepted for the fact that the present work utilizes the overall MG power balance, P_{BAL}, instead of only the electrical MG net power, P_{LG} as used in [11]. Taking into account this change and following the steps of [11], the grid power P_G^{S1} is computed according to the MG power balance, to its forecast error, and as well as to the current energy stored in the ESS. To do so P_G^{S1} is split into three components as:

$$P_G^{S1}(n) = P_{CTR}(n) + P_{SOC}(n) + P_{FLC,E}(n) \tag{12}$$

where the first component, P_{CTR}, is the average value between the MG overall power balance of the previous 12h, P_{BAL}^{12h}, and the forecast value of this balance for the next 12h, $P_{BAL}^{12h,FC}$, thus defined as:

$$P_{CTR}(n) = \frac{1}{2}\left[P_{BAL}^{12h}(n) + P_{BAL}^{12h,FC}(n)\right] \tag{13}$$

These values are computed by a CMA filter according to the expressions given in (14) and (15):

$$P_{BAL}^{12h}(n) = \frac{1}{M_{12}}\sum_{k=1}^{M_{12}}P_{BAL}(n-k) \tag{14}$$

$$P_{BAL}^{12h,FC}(n) = \frac{1}{M_{12}}\sum_{k=1}^{M_{12}}P_{BAL}^{FC}(n+k) \tag{15}$$

where M_{12} represents the number of samples in 12 hours.

The second component P_{SOC}, in (12) takes into account the SOC of the battery and is proportional to the difference between the reference SOC value, SOC_{REF}, and the average SOC value of the previous 24h, SOC_{AVG}:

$$P_{SOC}(n) = k_E\left[SOC_{REF} - SOC_{AVG}(n)\right] \tag{16}$$

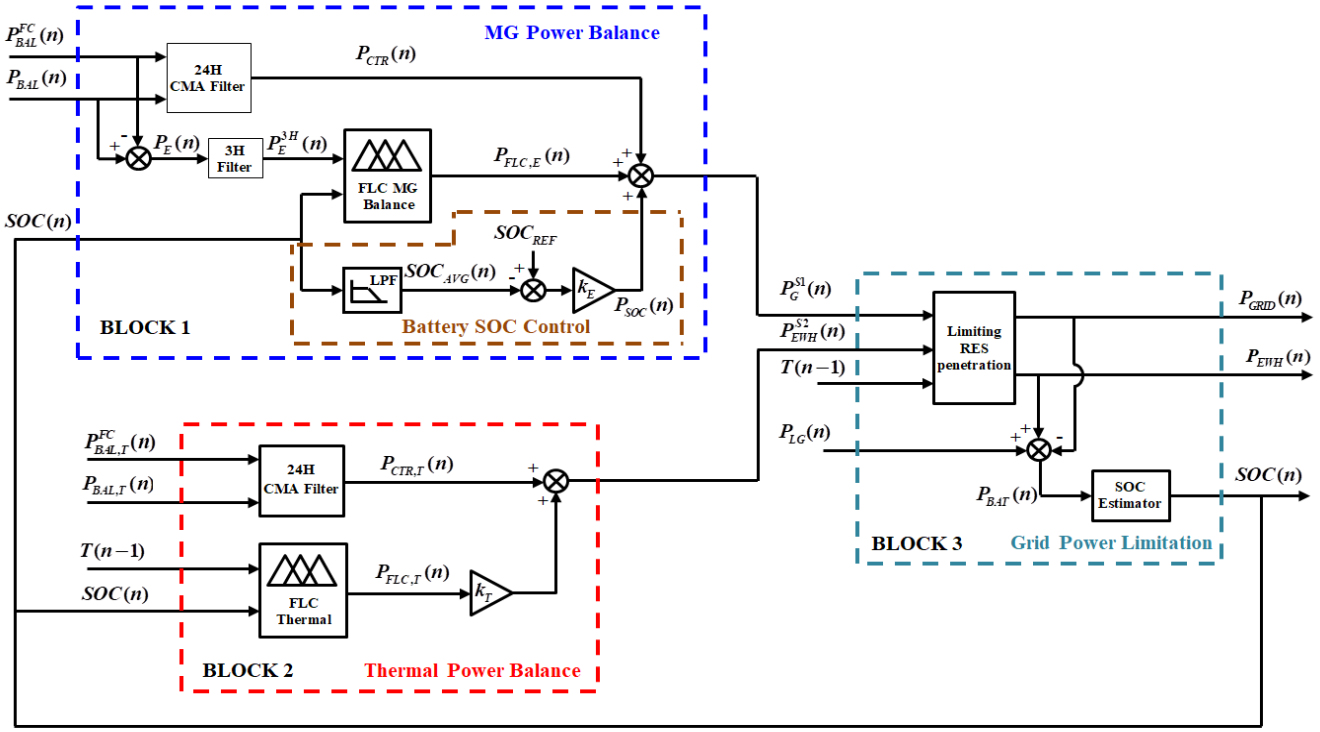

FIGURE 2. Complete block diagram of the proposed fuzzy-based EMS.

The average SOC value can be written further as:

$$SOC_{AVG}(n) = \frac{1}{M_{24}} \sum_{k=1}^{M_{24}} SOC(n-k) \tag{17}$$

where M_{24} represents the number of samples in 24 hours. This component is used to maintain the battery SOC fluctuating around to the 75% of the ESS rated capacity and not to drift away from this value. Note that the proportional gain, k_E, is therefore set to $k_E = 0.075$ kW/% in order to obtain high enough phase margin in the battery SOC loop control [11], [36].

Finally, the third variable in (12), $P_{FLC,E}$, is used to smooth the grid power profile P_G^{S1} depending on the current battery SOC and the forecast error of the MG power balance, $P_E = P_{BAL} - P_{BAL}^{FC}$ of the previous 3h, P_E^{3h}, which is defined as:

$$P_E^{3h}(n) = \frac{1}{M_3} \sum_{k=1}^{M_3} P_E(n-k) \tag{18}$$

where M_3 represents the number of samples in 3 hours. This component is computed by a two-input, one-output, and 25 rules FLC block that will be presented in Section V.

B. BLOCK 2: THERMAL POWER BALANCE – DEMAND MANAGEMENT

The second block in Fig.2 deals with the EWH demand management considering the MG thermal balance, $P_{BAL,T}$, defined as the difference between the DHW consumption, P_{DHW}, and the power generated by the solar collector, P_{SC},:

$$P_{BAL,T}(n) = P_{DHW}(n) - P_{SC}(n) \tag{19}$$

In short, this block determines the power required by the EWH in order to maintain the temperature in the water tank stable and in the chosen range.

The EWH power before the power clamper of Block 3, P_{EWH}^{S2}, is computed as the sum of two components, as follows:

$$P_{EWH}^{S2}(n) = P_{CTR,T}(n) + k_T \cdot P_{FLC,T}(n) \tag{20}$$

The first component $P_{CTR,T}$ is the average thermal power balance used to provide a low-frequency profile to the EWH power, namely:

$$P_{CTR,T}(n) = \frac{1}{2}\left[P_{BAL,T}^{12h}(n) + P_{BAL,T}^{12h,FC}(n)\right] \tag{21}$$

As for the Block 1, $P_{CTR,T}$ is computed by means of a CMA filter which uses the thermal power balance of the previous 12h, $P_{BAL,T}^{12h}$, and the forecast of the thermal power balance for the following 12h, $P_{BAL,T}^{12h,FC}$, defined as:

$$P_{BAL,T}^{12h}(n) = \frac{1}{M_{12}} \sum_{k=1}^{M_{12}} P_{BAL,T}(n-k) \tag{22}$$

$$P_{BAL,T}^{12h,FC}(n) = \frac{1}{M_{12}} \sum_{k=1}^{M_{12}} P_{BAL,T}^{FC}(n+k) \tag{23}$$

The second component of (20), $P_{FLC,T}$ is computed by means of a two-input, one output FLC block of 25 rules that

sets the amount of power supplied to the EWH according to the water temperature in the water tank and the battery SOC. Note that this component is proportional to the rated-power of EWH. In this work, the maximum power set by the FLC output is 75% of the EWH rated-power (i.e., $k_T = 0.75$) to avoid strong power variations in the EWH power profile. The FLC design will be presented further in Section V.

C. BLOCK 3: LIMITATION OF GRID POWER INJECTION

The third block in Fig.2 establishes the strategy to define the final values of both the grid power profile, P_{GRID}, and the power delivered to the EWH, P_{EWH}.

If the power, P_G^{S1} defined in Block 1 is less than the maximum injection power allowed to the utility grid, P_{LIM}, the proposed ESM sets the final grid power to P_{LIM} and transfers the excess power to the EWH as long as the water temperature in the tank is below the established upper limit, $T_{\max}^{iny}$.

Otherwise, the final grid power takes the value of the initial grid power ($P_{GRID} = P_G^{S1}$) if P_G^{S1} is greater than P_{LIM}, in order to limit the power injection from the MG to the mains. This strategy can be easily implemented by means of (24) to define the final grid power profile whereas the transfer of the power excess to the EWH is quantified by (25):

$$P_{GRID}(n) = \begin{cases} P_{LIM}, & if \;\; T(n) \le 65 \; AND \; P_G^{S1}(n) \le P_{LIM} \\ P_G^{S1}(n), & otherwise \end{cases} \tag{24}$$

$$P_{EWH}(n) = \begin{cases} P_{EWH}^{S1}(n) + \left| P_G^{S1}(n) + P_{LIM} \right|, \\ \quad if \begin{cases} T(n) \le T_{\max}^{iny} \\ \quad and \\ P_G^{S1}(n) \le P_{LIM} \end{cases} \\ P_{EWH}^{S2}(n), \quad otherwise \end{cases} \tag{25}$$

The case under study considers a maximum power injection to the mains of $P_{LIM} = -0.8$ kW and a maximum water temperature for power injection of $T_{\max}^{iny} = 70°C$. Finally, once the grid power profile and the EWH power are obtained, the power delivered/absorbed by the battery ESS can be computed by means of (2).

A complete flowchart of the proposed EMS, including the sequence of steps taken and their variables at the different levels, is presented in Fig. 3.

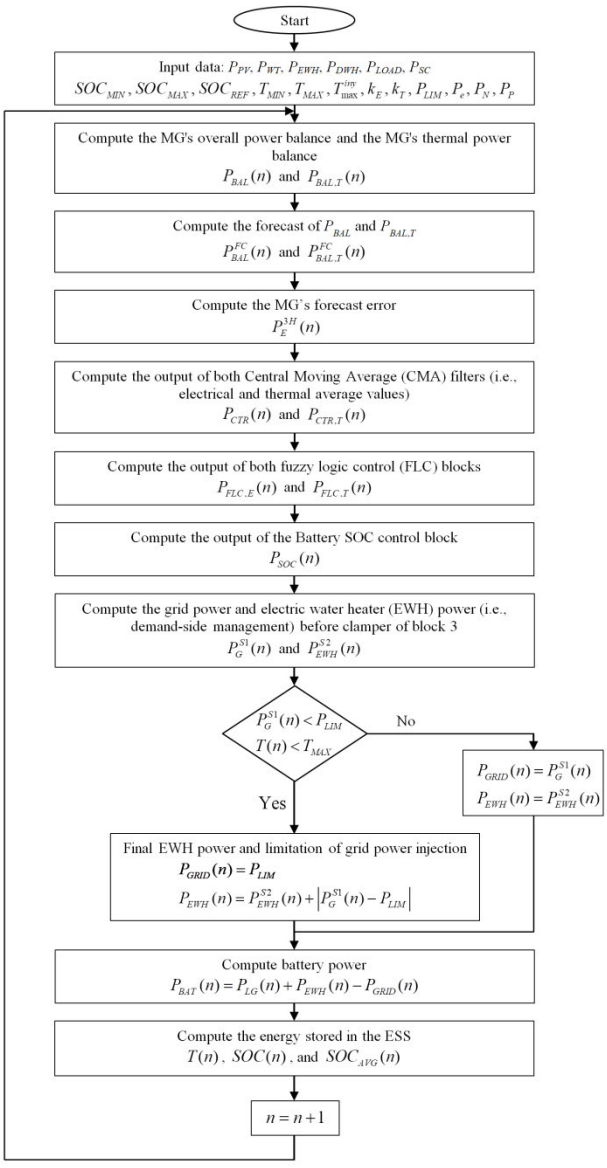

FIGURE 3. Flowchart of the proposed fuzzy-based energy management system.

V. FUZZY LOGIC CONTROLLERS DESIGN

The FLC blocks, shown in Fig. 2, assume a Mamdani-based inference and a defuzzification of Center of Gravity [41]. This study uses two FLC blocks, the first one, namely FLC MG balance, is used to smooth the grid power profile and the second one, namely FLC thermal, is used to determine the power assigned to the EWH.

The FLC design makes use of one year of real data obtained by measuring the output power of the RES as well as the load consumptions of the microgrid laboratory installed at Public University of Navarre, Navarra, Spain [10], [11], [35], [36], [45]. The data acquisition was carried out by means of power analyzers recording data every second and then obtaining the average of all variables every 15 minutes.

A. FLC MG BALANCE BLOCK

As mentioned in Section 4.1, this block computes the variable $P_{FLC,E}$ according to the magnitude of inputs P_E^{3h} and SOC. This FLC block follows the design and methodology presented by the authors in [10], [11], [44]. In this context, the FLC parameter adjustment, for instance, selection of membership functions (MF) number, type, mapping, and rule base, is performed by an offline adjustment procedure, which is described in [44] to minimize the magnitude of the defined quality criteria. Note that beside the procedure used in this

work, different methods to perform the parameter adjustment of the FLC controller can be used, for instance, metaheuristic nature-inspired algorithms (i.e., Cuckoo Search, Particle Swarm Optimization, among others) [53]–[55] or evolutionary algorithms (i.e., Genetic Algorithms, Machine Learning, among others) [42], [43].

As a result of the aforementioned procedure, five triangular MFs are assigned to both input variables whereas seven triangular MFs are assigned to the output variable. These MFs correspond to the fuzzy sub-sets denoted as NB for ''Negative Big'', NS for ''Negative Small'', NSS for ''Negative Smallest'', ZE for ''Zero'', PSS for ''Positive Smallest'', PS for ''Positive Small'', PM for ''Positive Medium'', and PB for ''Positive Big'', as shown in Fig. 4.

As it can be seen in Fig. 4, each variable has a pre-defined variation range. The variation range for input variable *SOC* (n) is defined by (4) whereas the variation range of input variable $P_E^{3h}(n)$ and output variable $P_{FLC,E}$ (n) are defined as follows:

$$-P_e \leq P_E^{3h}(n) \leq +P_e \tag{26}$$

$$P_N \leq P_{FLC,E}(n) \leq P_P \tag{27}$$

TABLE 2. Rule Base of the MG balance FLC block.

$P_{FLC,E}$		$P_E^{3h}(n)$				
		NB	**NS**	**ZE**	**PS**	**PB**
***SOC* (*n*)**	**NB**	PB	PM	NSS	NS	PB
	NS	PSS	PS	PSS	PS	PSS
	ZE	PB	PSS	PSS	PSS	PSS
	PS	NS	NSS	PS	NS	NS
	PB	NS	PSS	PM	NS	**NB**

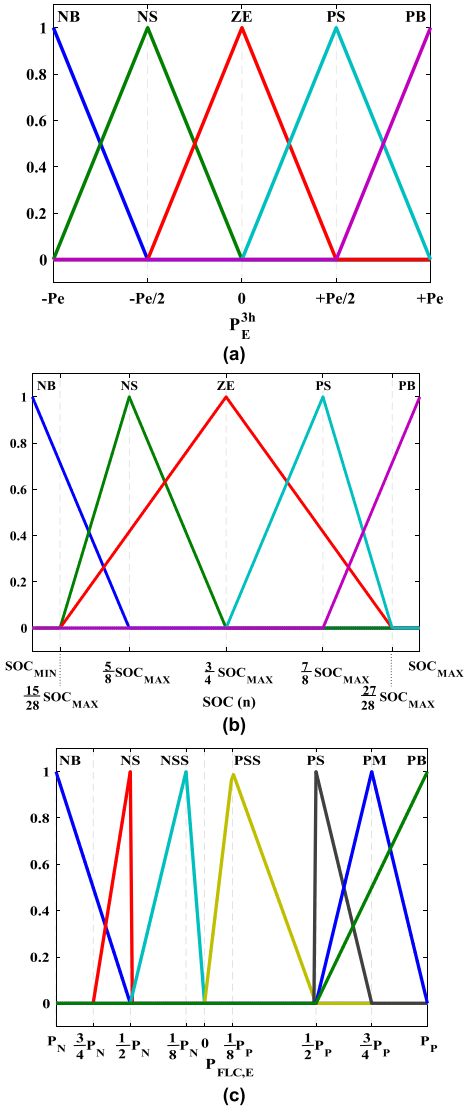

FIGURE 4. Membership functions for inputs and output variables of FLC MG balance block (a) input P_E^{3h}, (b) input *SOC*, and (c) output $P_{FLC,E}$.

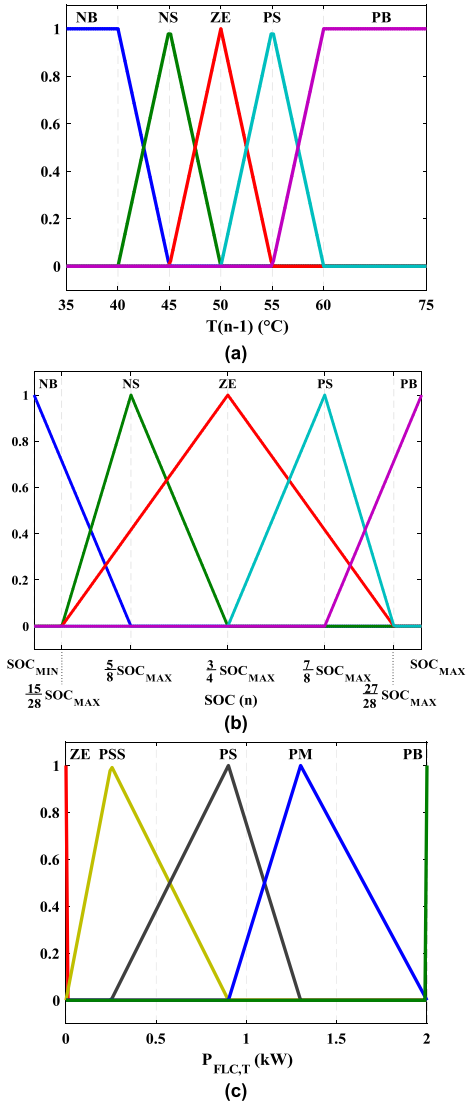

FIGURE 5. Membership functions for inputs and output variables of FLC thermal balance block (a) input T ($n-1$), (b) input *SOC*, and (c) output $P_{FLC,T}$.

TABLE 3. Rule base of the Thermal balance FLC block.

$P_{FLC,T}$		$T(n-1)$				
		NB	**NS**	**ZE**	**PS**	**PB**
$SOC\ (n)$	**NB**	PSS	ZE	ZE	ZE	ZE
	NS	PSS	ZE	ZE	ZE	ZE
	ZE	PSS	PSS	ZE	ZE	ZE
	PS	PM	PS	PS	PB	ZE
	PB	**PB**	PM	PS	PM	PM

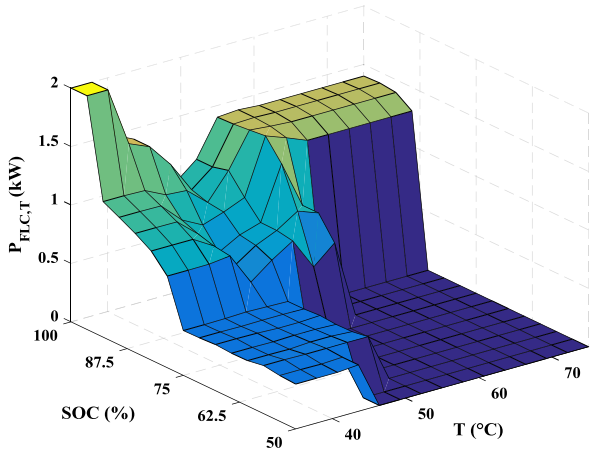

FIGURE 6. Surface plot of thermal balance fuzzy system input-output relationship.

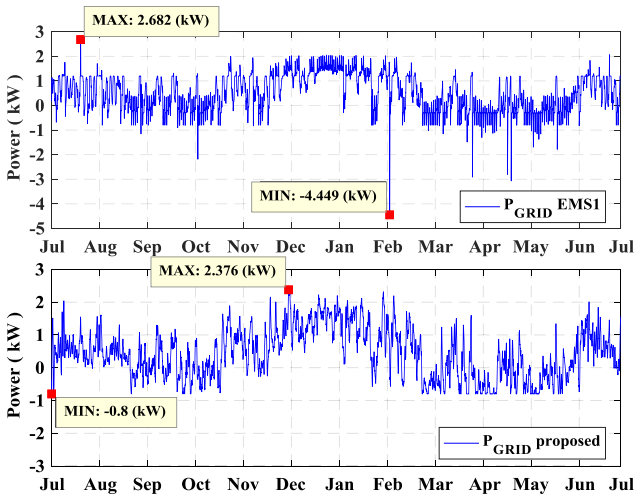

FIGURE 7. Power exchanged with the grid using EMS1 (top) and the proposed EMS strategy (bottom).

where P_e is the maximum error in the power balance forecast allowable in the MG, and P_N and P_P are the minimum and maximum power assigned to the FLC controller output, respectively. The case under study has considered the following values: $SOC_{MIN} = 50\%$, $SOC_{MAX} = 100\%$, $P_e = 6$ kW, $P_N = -0.3$ kW, and $P_P = 0.45$ kW [11].

Regarding the FLC rule base the adjustment procedure results in a set of rules which smooth the grid power profile

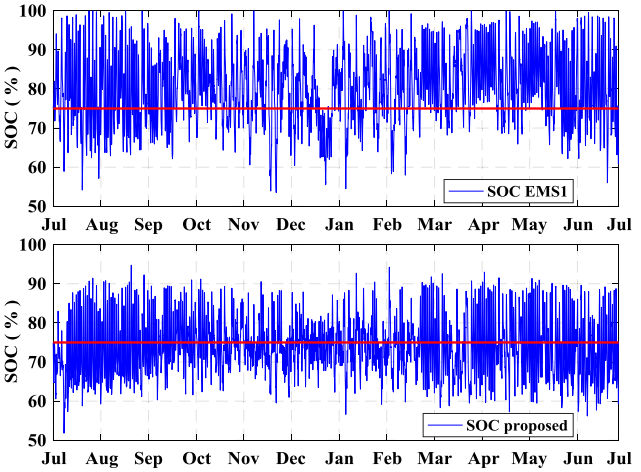

FIGURE 8. Comparison of the battery SOC profile between the EMS1 (top) and the proposed EMS strategy (bottom).

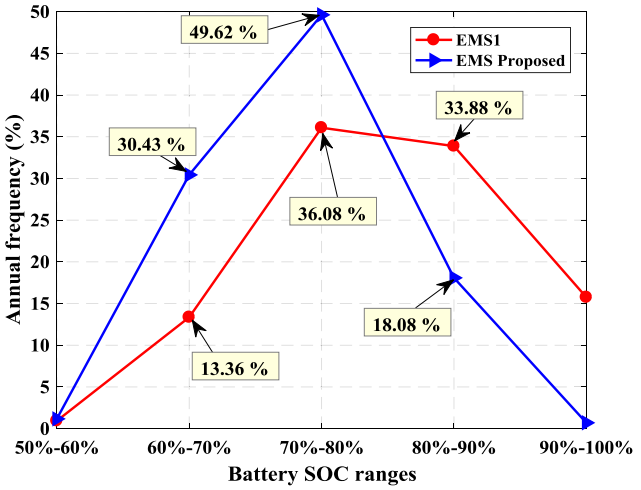

FIGURE 9. Histogram of the battery SOC ranges in the year under analysis for the EMS1 and the proposed EMS strategies.

and minimize the magnitude of the quality criteria defined in Section III. This rule base consists of 25 rules as presented in Table 2 which establishes the control policy. For instance, the last rule (highlighted in the table) is formulated as: ''IF the error, in the previous 3-h, of the MG power balance forecast is high, (i.e., the MG power balance is far greater than the forecasted value, $P_E^{3h}(n) \gg 0$), AND the energy stored in the battery ESS is high, (i.e., the $SOC\ (n)$ is close to SOC_{MAX}), THEN strongly increase the grid power to discharge the battery ESS, (i.e., $P_{FLC}\ (n) \ll 0$''), therefore, increasing the power injected to the mains.

B. FLC THERMAL BALANCE BLOCK

Similarly, the FLC design for the thermal balance block follows the aforementioned procedure [44]. The adjustment of the FLC parameters is performed only for the input $T\ (n-1)$ and the output $P_{FLC,T}$, since the input SOC is common for both FLC blocks. In short, five MFs (three triangular MFs

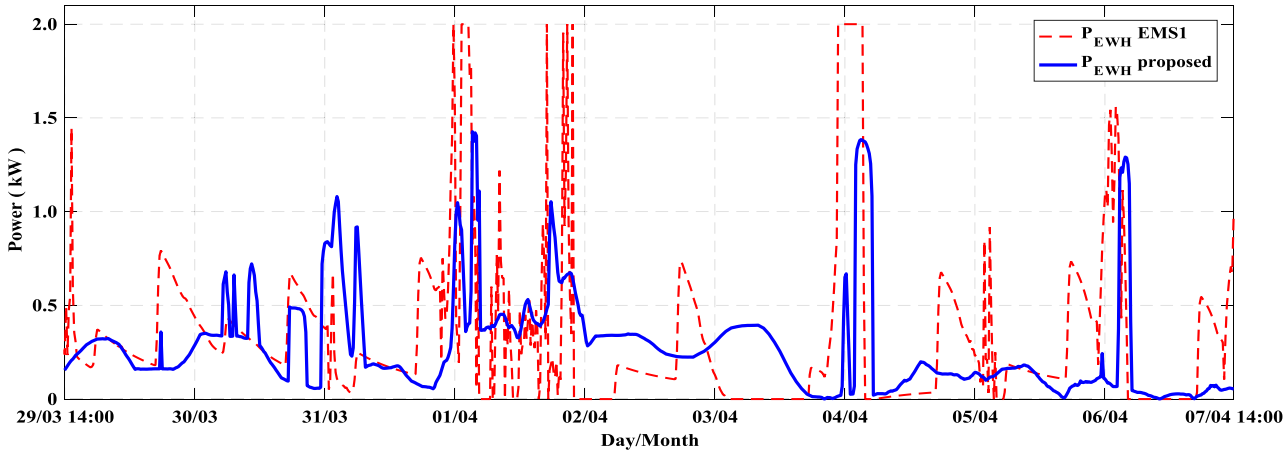

FIGURE 10. Electric water heater power P_{EWH} with EMS1 (red dotted line) and with the proposed EMS (blue solid line).

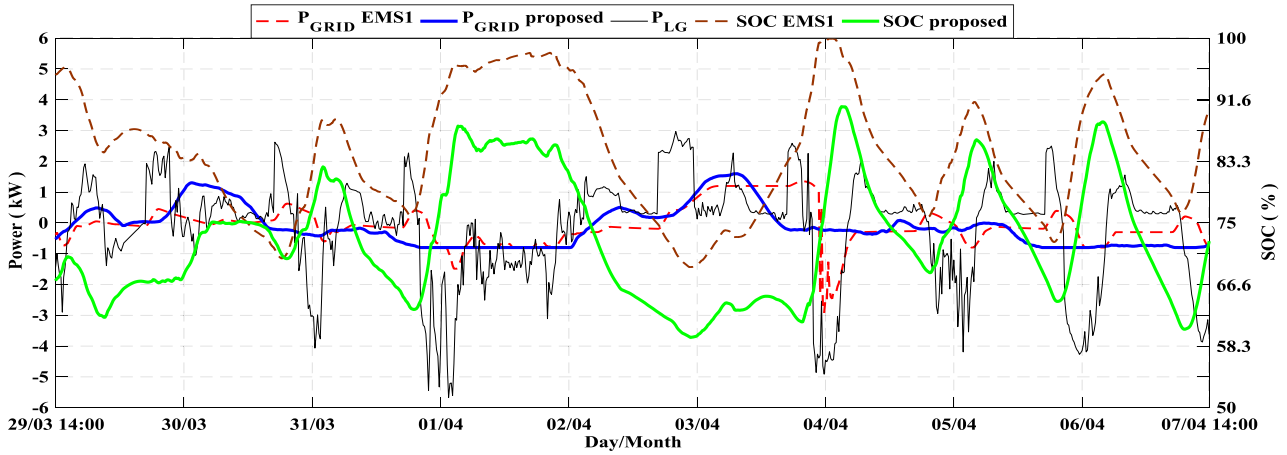

FIGURE 11. Simulation results for the grid power profile and the battery SOC with EMS1 and the proposed EMS.

and two trapezoidal MFs) are assigned to the input $T\ (n-1)$ and five MFs (three triangular MFs and two single tones) are assigned to the FLC output, as shown in Fig. 5. These MFs are distributed along the variation range of each variable, defined as:

$$35°C \leq T(n-1) \leq 75°C \tag{28}$$

$$0 \leq P_{FLC,T}(n) \leq 2kW \tag{29}$$

Following the same procedure, the rule base of the thermal balance FLC block consists of 25 rules that establish the power assigned to the EWH. As presented in Table 3, the highlighted cell is formulated as: "IF the temperature in the water tank is low, (i.e., $T\ (n-1) < 40°C$), AND the energy stored in the battery ESS is high, (i.e., $SOC\ (n)$ close to SOC_{MAX}), THEN strongly increase the power assigned to the EWH to increase the water temperature and to avoid the battery over charging.

Fig. 6 shows the surface of the thermal balance FLC block. As it can be seen, the power assigned to the EWH decreases as the water temperature increases, whereas it increases as the battery SOC increases. It is worth noting that the power assigned to the EWH is zero when the water temperature exceeds 50°C excepted when the battery charge is over 75% and should be limited.

VI. SIMULATION RESULTS AND COMPARISON

The simulation of the proposed EMS is performed using the one-year historical data recorded at the MG installed at the Public University of Navarre. The forecast of renewable power generation is estimated by Numerical Weather Prediction method [56] using the data provided by Meteo-Galicia THREDDS Server [57], which comprise a set of hourly weather data for the Iberian Peninsula that is updated every 12 hours with three days prediction horizon [11]. The forecast of load demand is obtained through the persistence model (i.e., the past data is the forecast for the next sampling time) [36]. Both the renewable power generation and the load forecasts are estimated using the MG power forecasting procedure presented in [11].

The simulation results are compared with the heuristic approach described in [35], referred to as EMS1. Fig. 7 shows the grid power profiles for both EMSs.

As shown in Fig. 7, the resulting grid power profile achieved by EMS 1 has still high power peaks due to inefficient energy management of the ESS, i.e., battery overcharging, as evidenced in Fig. 8. On Fig. 7 can be seen the proposed EMS performs a suitable management of the ESS and achieves a reduction in both the maximum power absorbed/injected from/to the utility network of 11.41% and 82.02%, respectively. The introduction of the power injection limitation in the EMS allows a maximum power fed into the grid of 0.8 kW, thus, removing the negative power peaks in the grid power profile.

In this regard, the enhanced behavior of the proposed EMS is also validated when comparing the battery SOC profile achieved by both EMSs, as shown in Fig. 8. The battery SOC evolution of the proposed EMS strategy exhibits less deviations with respect to 75% of the rated battery capacity (red solid line) by mitigating overcharge and over-discharge of the ESS. This mitigation is better visible on the histogram in Fig. 9 which quantifies the annual percentages of the time intervals when the battery SOC remains between prefixed limits for the considered year. As can be seen, the battery SOC remains in a range between 70% and 80% of the rated battery capacity during almost 50% (49.62%) of the year under analysis, improving the previous value achieved by the EMS1 (36.08%).

On Fig. 10 and Fig. 11 the resulting power of the EWH and the grid power profile together with the battery SOC along 4 days in April and acquired with both EMSs are presented.

As can be seen in Fig. 11, on April 4 the EMS1 strategy leads the battery's SOC to reach its allowed charge limit (brown dashed line in Fig. 10), which entails a power peak in the grid power profile (red dashed line in Fig. 11). Conversely, for the same date the proposed EMS performs better management of both the EWH power (blue solid line in Fig. 10) and the battery SOC (green solid line in Fig. 11). This improved behavior prevents the ESS overcharge and the subsequent power peaks in the network profile. Therefore a smoother grid power profile (blue solid line in Fig. 11) with fewer fluctuations is achieved. Note that the grid power profile on certain days (e.g., April 1st to 2nd in Fig. 11) is constant, although the MG net power (black dotted line in Fig. 11) is highly variable.

Table 4 summarizes the resulting values of the aforementioned quality criteria to the grid power profile achieved by both EMSs. Note that for comparison purposes the values of the quality criteria obtained for the case of a MG without an EMS (i.e., $P_{GRID} = P_{LG}$) is also included in Table 4. It is worth pointing out that the proposed EMS reduces all defined quality criteria, some of them more significantly than others. The MPD criterion is very much lowered down, actually by 96% compared with the EMS1 due to the inclusion of the power clamper block.

TABLE 4. Quality criteria comparison.

EMS	$P_{G,MAX}$ (kW)	$P_{G,MIN}$ (kW)	*MPD* (W/h)	*APD* (W/h)	*PPV*
No EMS	6.53	-6.45	18468	1222	13.3
EMS1 [35]	2.68	-4.45	19022	84.02	1.23
Proposed EMS	2.38	-0.8	352	59.11	1.24

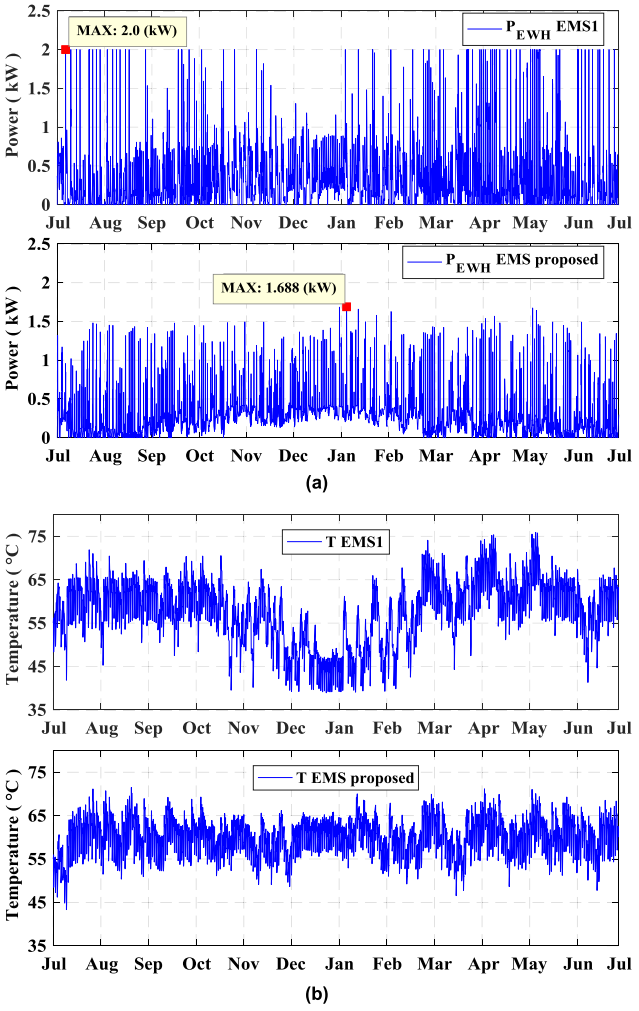

FIGURE 12. Comparison of simulation results (EMS1 (top) and proposed EMS (bottom)) (a) electric water heater power and (b) water temperature in the storage tank.

Finally, Fig. 12(a) and Fig. 12(b) present the EWH power profile and the temperature of the water tank, respectively, achieved by both EMSs along the year under analysis. As can be seen, the maximum power used by the EWH with the proposed EMS is 1.688 kW, while it is 2 kW for the EMS1. The temperature in the water tank is kept between the established limits in both cases (35°C and 75°C), however showing less fluctuations in the case of the proposed EMS.

VII. CONCLUSION

This paper has addressed the design of a fuzzy-based energy management system for grid profile smoothing of

a residential grid-connected electro-thermal microgrid. The EMS has been designed based on FLC to smooth the power profile exchanged with the grid and limiting the injection of RES into the mains. The EMS design has been built out of three blocks, where the first one uses a FLC block to compute the preliminary value of the grid power profile according to the error in the MG power balance forecast and the battery SOC; the second block performs a demand-side management of the EWH through the use of another FLC block and accounting for the MG thermal balance and the water temperature in the thermal storage (water tank); the third block is used to define the final values of the grid power profile and the EWH power and performs the limitation of the RES penetration into the grid. Analysis of the comparative simulations with a similar heuristically approach has demonstrated the improved features of the proposed EMS. These results can be summarized as:

- An improvement on the grid power profile smoothness, by reducing the maximum and minimum values of the power injected/fed from/to the grid.
- A less fluctuating EWH power consumption profile with a lower maximum value.
- A battery SOC profile with lower fluctuations centered to the 75% of the battery rated capacity. This reduction would allow a lower sizing of the ESS compared with the use of a SMA filter.

From a quantitative point of view, with respect to the heuristically EMS, the proposed EMS approach has featured a 11.4% reduction of the maximum power absorbed from the grid as well as a very significant reduction of 98% of the MPD criterion concerning the grid power fluctuations. Further, it can be pointed out that these improved features of the proposed EMS have been obtained including a grid power clamper block allowing the grid power injection limitation to a desired upper limit, which was not considered in the strategy EMS1. For the case under study, this limit has allowed a reduction of 82.02% of the maximum power value injected to the grid.

The authors consider that the proposed approach can be classified as a ''low computational complexity'' one due to the simplicity of the off-line trained fuzzy controllers and can be embedded in low cost digital platforms as it was done in [11].

As a critical discussion, one the possible drawbacks of the proposed approach is the availability of historical data along one year mainly on the consumption side, since environmental variables and predictions for RES production are accessible in public databases. However, in the framework of current and future policies to reduce the fossil fuel dependence in electricity generation, metering at user level is expected to play a key role [58]. On the other hand, building and comparing different on-line optimization strategies as those cited in Table 1 and recent works of more theoretical aspects on FLC design [59], [60] applied to the scenario and the goals of this work would be also interesting. They can contribute to establish a trade-off between computational complexity and resulting grid profiles. Finally, including economic variables in the optimization process and analyzing the resulting grid profiles would also provide useful assessments on tariff policies and their feasibility. All these issues would be undertaken in a future work.

REFERENCES

[1] M. Karmellos, P. N. Georgiou, and G. Mavrotas, "A comparison of methods for the optimal design of distributed energy systems under uncertainty," *Energy*, vol. 178, pp. 318–333, Jul. 2019.

[2] International Energy Agency, "CO_2 emissions from fuel combustion 2018," OECD, Paris, France, Tech. Rep., Oct. 2018, doi: 10.1787/co2_fuel-2018-en.

[3] X. Shi, A. Dini, Z. Shao, N. H. Jabarullah, and Z. Liu, "Impacts of photovoltaic/wind turbine/microgrid turbine and energy storage system for bidding model in power system," *J. Cleaner Prod.*, vol. 226, pp. 845–857, Jul. 2019.

[4] G. Brunaccini, F. Sergi, D. Aloisio, N. Randazzo, M. Ferraro, and V. Antonucci, "Fuel cells hybrid systems for resilient microgrids," *Int. J. Hydrogen Energy*, vol. 44, no. 38, pp. 21162–21173, Aug. 2019.

[5] A. Hirsch, Y. Parag, and J. Guerrero, "Microgrids: A review of technologies, key drivers, and outstanding issues," *Renew. Sustain. Energy Rev.*, vol. 90, pp. 402–411, Jul. 2018.

[6] M. F. Zia, E. Elbouchikhi, and M. Benbouzid, "Microgrids energy management systems: A critical review on methods, solutions, and prospects," *Appl. Energy*, vol. 222, pp. 1033–1055, Jul. 2018.

[7] D. Espín-Sarzosa, R. Palma-Behnke, and O. Núñez-Mata, "Energy management systems for microgrids: Main existing trends in centralized control architectures," *Energies*, vol. 13, no. 3, p. 547, Jan. 2020.

[8] R. H. Lasseter, "MicroGrids," in *Proc. Power Eng. Soc. Winter Meeting*, vol. 1, Jan. 2002, pp. 305–308.

[9] N. Hatziargyriou, H. Asano, R. Iravani, and C. Marnay, "Microgrids," *IEEE Power Energy Mag.*, vol. 5, no. 4, pp. 78–94, Jul./Aug. 2007.

[10] D. Arcos-Aviles, J. Pascual, L. Marroyo, P. Sanchis, and F. Guinjoan, "Fuzzy logic-based energy management system design for residential grid-connected microgrids," *IEEE Trans. Smart Grid*, vol. 9, no. 2, pp. 530–543, Mar. 2018.

[11] D. Arcos-Aviles, J. Pascual, F. Guinjoan, L. Marroyo, P. Sanchis, and M. P. Marietta, "Low complexity energy management strategy for grid profile smoothing of a residential grid-connected microgrid using generation and demand forecasting," *Appl. Energy*, vol. 205, pp. 69–84, Nov. 2017.

[12] B. V. Solanki, C. A. Canizares, and K. Bhattacharya, "Practical energy management systems for isolated microgrids," *IEEE Trans. Smart Grid*, vol. 10, no. 5, pp. 4762–4775, Sep. 2019.

[13] A. C. Z. de Souza, F. M. Portelinha, D. Marujo, and D. Q. Oliveira, "Microgrids operation in islanded mode," in *Sustainable Development in Energy Systems*. Cham, Switzerland: Springer, 2017, ch. 10, pp. 193–215.

[14] Y. E. G. Vera, R. Dufo-López, and J. L. Bernal-Agustín, "Energy management in microgrids with renewable energy sources: A literature review," *Appl. Sci.*, vol. 9, no. 18, p. 3854, Sep. 2019.

[15] A. Cagnano, E. De Tuglie, and P. Mancarella, "Microgrids: Overview and guidelines for practical implementations and operation," *Appl. Energy*, vol. 258, Jan. 2020, Art. no. 114039.

[16] M. A. Mahmud, M. J. Hossain, H. R. Pota, and A. B. M. Nasiruzzaman, "Voltage control of distribution networks with distributed generation using reactive power compensation," in *Proc. 37th Annu. Conf. IEEE Ind. Electron. Soc. (IECON)*, Melbourne, VIC, Australia, Nov. 2011, pp. 985–990.

[17] T. Krechel, F. Sanchez, F. Gonzalez-Longatt, H. Chamorro, and J. L. Rueda, "Transmission system-friendly microgrids: An option to provide ancillary services," in *Distributed Energy Resources in Microgrids*. Amsterdam, The Netherlands: Elsevier, 2019, pp. 291–321.

[18] J. Black and R. Larson, "Strategies to overcome network congestion in infrastructure systems," *J. Ind. Syst. Eng.*, vol. 1, no. 2, pp. 97–115, 2007.

[19] X. Li, X. Cao, C. Li, B. Yang, M. Cong, and D. Chen, "A coordinated peak shaving strategy using neural network for discretely adjustable energy-intensive load and battery energy storage," *IEEE Access*, vol. 8, pp. 5331–5338, 2020.

[20] A. A. Bashir, M. Pourakbari-Kasmaei, J. Contreras, and M. Lehtonen, "A novel energy scheduling framework for reliable and economic operation of islanded and grid-connected microgrids," *Electr. Power Syst. Res.*, vol. 171, pp. 85–96, Jun. 2019.

[21] J. Wu, X. Xing, X. Liu, J. M. Guerrero, and Z. Chen, "Energy management strategy for grid-tied microgrids considering the energy storage efficiency," *IEEE Trans. Ind. Electron.*, vol. 65, no. 12, pp. 9539–9549, Dec. 2018.

[22] C. Zhang, Y. Xu, Z. Y. Dong, and K. P. Wong, "Robust coordination of distributed generation and price-based demand response in microgrids," *IEEE Trans. Smart Grid*, vol. 9, no. 5, pp. 4236–4247, Sep. 2018.

[23] A. H. Sharifi and P. Maghouli, "Energy management of smart homes equipped with energy storage systems considering the PAR index based on real-time pricing," *Sustain. Cities Soc.*, vol. 45, pp. 579–587, Feb. 2019.

[24] A. Anvari-Moghaddam, J. M. Guerrero, J. C. Vasquez, H. Monsef, and A. Rahimi-Kian, "Efficient energy management for a grid-tied residential microgrid," *IET Gener., Transmiss. Distrib.*, vol. 11, no. 11, pp. 2752–2761, Aug. 2017.

[25] C. L. Nge, I. U. Ranaweera, O.-M. Midtgård, and L. Norum, "A real-time energy management system for smart grid integrated photovoltaic generation with battery storage," *Renew. Energy*, vol. 130, pp. 774–785, Jan. 2019.

[26] C. Zhang, W. Lin, D. Ke, and Y. Sun, "Smoothing tie-line power fluctuations for industrial microgrids by demand side control: An output regulation approach," *IEEE Trans. Power Syst.*, vol. 34, no. 5, pp. 3716–3728, Sep. 2019.

[27] E. Yao, P. Samadi, V. W. S. Wong, and R. Schober, "Residential demand side management under high penetration of rooftop photovoltaic units," *IEEE Trans. Smart Grid*, vol. 7, no. 3, pp. 1597–1608, May 2016.

[28] M. Vahedipour-Dahraie, H. Rashidizadeh-Kermani, A. Anvari-Moghaddam, and J. M. Guerrero, "Stochastic risk-constrained scheduling of renewable-powered autonomous microgrids with demand response actions: Reliability and economic implications," *IEEE Trans. Ind. Appl.*, vol. 56, no. 2, pp. 1882–1895, Mar. 2020.

[29] M. S. H. Nizami, M. J. Hossain, B. M. R. Amin, and E. Fernandez, "A residential energy management system with bi-level optimization-based bidding strategy for day-ahead bi-directional electricity trading," *Appl. Energy*, vol. 261, Mar. 2020, Art. no. 114322.

[30] I. R. S. da Silva, R. D. A. L. Rabêlo, J. J. P. C. Rodrigues, P. Solic, and A. Carvalho, "A preference-based demand response mechanism for energy management in a microgrid," *J. Cleaner Prod.*, vol. 255, May 2020, Art. no. 120034.

[31] D. Tenfen and E. C. Finardi, "A mixed integer linear programming model for the energy management problem of microgrids," *Electr. Power Syst. Res.*, vol. 122, pp. 19–28, May 2015.

[32] T. Shekari, A. Gholami, and F. Aminifar, "Optimal energy management in multi-carrier microgrids: An MILP approach," *J. Modern Power Syst. Clean Energy*, vol. 7, no. 4, pp. 876–886, Jul. 2019.

[33] N. Bazmohammadi, A. Anvari-Moghaddam, A. Tahsiri, A. Madary, J. C. Vasquez, and J. M. Guerrero, "Stochastic predictive energy management of multi-microgrid systems," *Appl. Sci.*, vol. 10, no. 14, p. 4833, Jul. 2020.

[34] X. Hou, J. Wang, T. Huang, T. Wang, and P. Wang, "Smart home energy management optimization method considering energy storage and electric vehicle," *IEEE Access*, vol. 7, pp. 144010–144020, 2019.

[35] J. Pascual, P. Sanchis, and L. Marroyo, "Implementation and control of a residential electrothermal microgrid based on renewable energies, a hybrid storage system and demand side management," *Energies*, vol. 7, no. 1, pp. 210–237, Jan. 2014.

[36] J. Pascual, J. Barricarte, P. Sanchis, and L. Marroyo, "Energy management strategy for a renewable-based residential microgrid with generation and demand forecasting," *Appl. Energy*, vol. 158, pp. 12–25, Nov. 2015.

[37] S. Zhang and Y. Tang, "Optimal schedule of grid-connected residential PV generation systems with battery storages under time-of-use and step tariffs," *J. Energy Storage*, vol. 23, pp. 175–182, Jun. 2019.

[38] S.-K. Kim, J.-H. Jeon, C.-H. Cho, J.-B. Ahn, and S.-H. Kwon, "Dynamic modeling and control of a grid-connected hybrid generation system with versatile power transfer," *IEEE Trans. Ind. Electron.*, vol. 55, no. 4, pp. 1677–1688, Apr. 2008.

[39] H. Zhou, T. Bhattacharya, D. Tran, T. S. T. Siew, and A. M. Khambadkone, "Composite energy storage system involving battery and ultracapacitor with dynamic energy management in microgrid applications," *IEEE Trans. Power Electron.*, vol. 26, no. 3, pp. 923–930, Mar. 2011.

[40] J. J. Barricarte, I. S. Martín, P. Sanchis, and L. Marroyo, "Energy management strategies for grid integration of microgrids based on renewable energy sources," in *Proc. 10th Int. Conf. Sustain. Energy Technol.*, Istambul, Turkey, Sep. 2011, pp. 4–7.

[41] K. Passino and S. Yurkovich, *Fuzzy Control*. Menlo Park, CA, USA: Addisson-Wesley, 1998.

[42] S. Leonori, A. Martino, F. M. F. Mascioli, and A. Rizzi, "Microgrid energy management systems design by computational intelligence techniques," *Appl. Energy*, vol. 277, Nov. 2020, Art. no. 115524.

[43] S. Leonori, M. Paschero, F. M. F. Mascioli, and A. Rizzi, "Optimization strategies for microgrid energy management systems by genetic algorithms," *Appl. Soft Comput.*, vol. 86, Jan. 2020, Art. no. 105903.

[44] D. A. Aviles, F. Guinjoan, J. Barricarte, L. Marroyo, P. Sanchis, and H. Valderrama, "Battery management fuzzy control for a grid-tied microgrid with renewable generation," in *Proc. 38th Annu. Conf. IEEE Ind. Electron. Soc. (IECON)*, Montreal, QC, Canada, Oct. 2012, pp. 5607–5612.

[45] D. Arcos-Aviles, F. Guinjoan, J. Pascual, L. Marroyo, P. Sanchis, R. Gordillo, P. Ayala, and M. P. Marietta, "A review of fuzzy-based residential grid-connected microgrid energy management strategies for grid power profile smoothing," in *Energy Sustainability in Built and Urban Environments*, E. Motoasca, A. K. Agarwal, and H. Breesch, Eds. Singapore: Springer, 2019, ch. 8, pp. 165–199.

[46] D. Arcos-Aviles, F. Guinjoan, J. Pascual, L. Marroyo, R. Gordillo, P. Sanchis, M. P. Marietta, and A. Ibarra, "Fuzzy-based energy management of a residential electro-thermal microgrid based on power forecasting," in *Proc. 44th Annu. Conf. IEEE Ind. Electron. Soc. (IECON)*, Washington, DC, USA, Oct. 2018, pp. 1824–1829.

[47] D. Arcos-Aviles, D. Sotomayor, J. L. Proano, F. Guinjoan, M. P. Marietta, J. Pascual, L. Marroyo, and P. Sanchis, "Fuzzy energy management strategy based on microgrid energy rate-of-change applied to an electro-thermal residential microgrid," in *Proc. IEEE 26th Int. Symp. Ind. Electron. (ISIE)*, Edinburgh, U.K., Jun. 2017, pp. 99–105.

[48] S. Anuphappharadorn, S. Sukchai, C. Sirisamphanwong, and N. Ketjoy, "Comparison the economic analysis of the battery between lithium-ion and lead-acid in PV stand-alone application," *Energy Procedia*, vol. 56, pp. 352–358, Jan. 2014.

[49] S. A. Kalogirou, *Solar Energy Engineering Processes and Systems*. Burlington, MA, USA: Elsevier, 2009.

[50] Energy Regulatory Commission. (Nov. 2016). *Philippine Distribution Code 2016 Edition*. [Online]. Available: http://www.erc.gov.ph/Files/Render/media/PhilippineDistributionCode2016Edition.pdf

[51] AEMC, "National electricity rules version 56 chapter 3: Market rules," Aust. Energy Mark., 2013, p. 146. [Online]. Available: https://www.aemc.gov.au/sites/default/files/content/National-Electricity-Rules-historical-version-79.pdf

[52] R. G. C. Secretariat. (2012). *Grid Connection Code for Renewable Power Plants (RPPs) Connected to the Electricity Transmission System (TS) or the Distribution System (DS) in South Africa*. [Online]. Available: http://www.nersa.org.za/Admin/Document/Editor/file/Electricity/TechnicalStandards/SouthAfricanGridCodeRequirementsforRenewablePowerPlants-Vesion26.pdf

[53] G. García-Gutiérrez, D. Arcos-Aviles, E. V. Carrera, F. Guinjoan, A. Ibarra, and P. Ayala, "The Cuckoo Search algorithm applied to fuzzy logic control parameter optimization," in *Applications of Cuckoo Search Algorithm and its Variants*, N. Dey, Ed. Singapore: Springer, 2021, ch. 8, pp. 175–206.

[54] D. Arcos-Aviles, G. Garcia-Gutierrez, F. Guinjoan, E. V. Carrera, J. Pascual, P. Ayala, L. Marroyo, and E. Motoasca, "Adjustment of the fuzzy logic controller parameters of the energy management strategy of a grid-tied domestic electro-thermal microgrid using the cuckoo search algorithm," in *Proc. 45th Annu. Conf. IEEE Ind. Electron. Soc. (IECON)*, Lisbon, Portugal, Oct. 2019, pp. 279–285.

[55] S. Berrazouane and K. Mohammedi, "Parameter optimization via cuckoo optimization algorithm of fuzzy controller for energy management of a hybrid power system," *Energy Convers. Manage.*, vol. 78, pp. 652–660, Feb. 2014.

[56] C. Yang, A. A. Thatte, and L. Xie, "Multitime-scale data-driven spatio-temporal forecast of photovoltaic generation," *IEEE Trans. Sustain. Energy*, vol. 6, no. 1, pp. 104–112, Jan. 2015.

[57] Meteogalicia. *Servidor THREDDS de MeteoGalicia*. Accessed: Jul. 5, 2018. [Online]. Available: http://www.meteogalicia.es/web/index.action

[58] European Commission. *Energy Efficiency First: Accelerating Towards a 2030 Objective of 32.5%*. Accessed: Jan. 13, 2021. [Online]. Available: https://ec.europa.eu/info/news/energy-efficiency-first-accelerating-towards-2030-objective-2019-sep-25_en

[59] E. Babaee Tirkolaee, A. Goli, and G.-W. Weber, "Fuzzy mathematical programming and self-adaptive artificial fish swarm algorithm for Just-in-Time energy-aware flow shop scheduling problem with outsourcing option," *IEEE Trans. Fuzzy Syst.*, vol. 28, no. 11, pp. 2772–2783, Nov. 2020.

[60] T. Garai and H. Garg, "Multi-objective linear fractional inventory model with possibility and necessity constraints under generalised intuitionistic fuzzy set environment," *CAAI Trans. Intell. Technol.*, vol. 4, no. 3, pp. 175–181, Sep. 2019.

DIEGO ARCOS-AVILES (Member, IEEE) was born in Quito, Ecuador, in 1978. He received the B.Sc. degree in electronics, automation and control engineering from the Universidad de las Fuerzas Armadas ESPE, Sangolquí, Ecuador, in 2002, and the M.Sc. and Ph.D. degrees in electronics engineering from the Universitat Politècnica de Catalunya, Barcelona, Spain, in 2012 and 2016, respectively.

He is currently an Associate Professor with the Department of Electrical, Electronics, and Telecommunications Engineering, Universidad de las Fuerzas Armadas ESPE, since 2002. Since 2017, he has been the Coordinator of the Research Group of Propagation, Electronics Control, and Networking (PROCONET). He is the Coordinator of the master's degree program in electronics since 2019. He has been involved in many research projects related to microgrids, power electronics, automation of industrial processes, control systems applications, and control of power electronics. His research interests energy management systems, microgrids, power electronics, smart grids, and renewable generation systems.

Dr. Arcos-Aviles is the Editor-in-Chief of *Maskay Journal*.

JULIO PASCUAL (Member, IEEE) was born in Pamplona in 1985. He received the B.Sc., M.Sc., and Ph.D. degrees in electrical engineering from the Public University of Navarre (UPNA), Pamplona, Spain, in 2011, 2012, and 2016, respectively. He did his last undergraduate year in Windsor, Canada, and then did his Final Project in close collaboration with the research group INGEPER (Electrical Engineering, Power Electronics and Renewable Energies) at UPNA, regarding flexible multijunction PV modules.

In 2011, he was hired as a Researcher for INGEPER, where he worked mainly on Energy Management Strategies for microgrids, which was the central topic of his Ph.D. thesis. During this period, he co-founded the student's association for renewable energies APERNA. Afterward, he continued his research activity in INGEPER, focusing on microgrids, residential PV systems and PV plants performance analysis. During his research period, he has participated in nine public and 12 private research projects; author of seven papers in international journals; and has contributed to 13 international conferences. During his first stage of his research period, he was also a Teaching Assistant until 2017, when he became an Assistant Professor at UPNA.

FRANCESC GUINJOAN (Member, IEEE) received the Ingeniero de Telecomunicación and the Doctor Ingeniero de Telecomunicación degrees from the Universitat Politècnica de Catalunya (UPC), Barcelona, Spain, in 1984 and 1990, respectively, and the Docteur es Sciences degree from the Université Paul Sabatier, Toulouse, France, in 1992.

He is currently a Full Professor at the Departamento de Ingenieria Electrónica, Escuela Técnica Superior de Ingenieros de Telecomunicación de Barcelona, UPC. His research interests include power electronics modeling and control for renewable energy systems. He has coauthored more than 90 papers in international journals and conference proceedings. Since 2005, he has been managing research projects evaluations in the field of electrical engineering as a member of the Spanish Research Agency (AEI), Ministry for Science, Innovation, and Universities. Since 2014, he has been the Delegate of the UPC and a member of the Supervisory Board of the Knowledge Innovation Community (KIC) Innoenergy, funded by the European Institute of Technology (EIT) of the European Union. He was a Guest Co-Editor of the Special Issue on Smart Devices for Renewable Energy Systems of the IEEE TRANSACTIONS ON INDUSTRIAL ELECTRONICS, in 2011.

LUIS MARROYO (Member, IEEE) received the M.Sc. degree in electrical engineering from the University of Toulouse, France, in 1993, and the Ph.D. degree in electrical engineering from the UPNA, Spain, and the LEEI-ENSEEIHT INP Toulouse, France, in 1997 and 1999, respectively.

From 1993 to 1998, he was an Assistant Professor at the Department of Electrical and Electronic Engineering, UPNA, where he currently works as an Associate Professor since 1998. He has been the Head of the INGEPER Research Group. He has been involved in more than 90 research projects mainly in co-operation with industry. He is the co-inventor of 23 international patents and has coauthored more than 100 papers in international journals and conferences. His research interests include power electronics, grid quality, and renewable energy.

GABRIEL GARCÍA-GUTIÉRREZ was born in Quito, Ecuador, in 1994. He received the B.Sc. degree in electronics, automation and control engineering from the Universidad de las Fuerzas Armadas ESPE, Sangolquí, Ecuador, in 2019.

He worked as a Research Assistant with the Research Group of Propagation, Electronic Control, and Networking (PROCONET), Universidad de las Fuerzas Armadas ESPE. His research interests include optimization, control theory, power electronics, and renewable generation systems.

RODOLFO GORDILLO-ORQUERA received the B.Sc. degree in electronic and telecommunications engineering and the master's degree in electronics engineering from the Universidad de las Fuerzas Armadas ESPE, Ecuador, in 1996 and 2008, respectively, and the Ph.D. degree in information and communication technology from Rey Juan Carlos University, Madrid, Spain, in 2019.

Since 1996, he has been carrying out research and teaching activities with the Department of Electric, Electronics and Telecommunications, ESPE. His research currently focuses on data-driven science, machine learning, and dynamical systems, and their applications in system identification, forecasting, and control.

JACQUELINE LLANOS-PROAÑO (Member, IEEE) received the B.Sc. and Engineer degrees in electronic engineering from the Army Polytechnic School, Ecuador, and the M.Sc. and Ph.D. degrees in electrical engineering from the University of Chile, Santiago. She is currently an Assistant Professor with the Department of Electrical and Electronics, Universidad de las Fuerzas Armadas ESPE, Ecuador. Her current research interests include control and management of microgrids, control of power generation plants, and predictive control.

PABLO SANCHIS (Senior Member, IEEE) received the M.Sc. degree in electrical engineering, the M.Sc. degree in management and business administration, and the Ph.D. degree in electrical engineering from the Public University of Navarre (UPNA), Pamplona, Spain, in 1994, 1995, and 2002, respectively.

From 1996 to 1998, he was a Guest Researcher with the Delft University of Technology, Delft, The Netherlands. In 1998, he joined the Department of Electrical, Electronic and Communications Engineering, Public University of Navarre, where he is also a Professor. He was the Vice Dean of the School of Industrial & ICT Engineering and the Director of the University Unit for Research Resources and Structures. He is currently the Director of the UPNA Chair for Renewable Energies and the Head of the Research Group in Electrical Engineering, Power Electronics, and Renewable Energies. He has been involved in more than 90 research projects both with public funding and in cooperation with industry and is the co-inventor of nine patents. He has supervised 10 Ph.D. theses and coauthored more than 140 articles and contributions in international journals and conferences as well as five book chapters (h-index of 31). His current research interests include renewable energies, power electronics, electric energy storage technologies, grid integration of renewable energies, and electric microgrids.

Dr. Sanchis received the UPNA Research Award for the Best Technical Paper in 2013 and the UPNA Excellence in Teaching Award in 2017.

T. EMILIA MOTOASCA was born in Brasov, Romania, in 1971. She received the B.S. and M.S. degrees in electrical engineering and in economics from the Transylvania University of Brasov, Romania, in 1997, and the Ph.D. degree in electrical engineering from the Delft University of Technology, The Netherlands, in 2003.

From 2003 to 2013, she worked as a Researcher and as an Assistant Professor with the Eindhoven University of Technology, The Netherlands. Since 2013, she has been working with KU Leuven - Technology campus Ghent, Belgium, from 2013 to 2020. Recently, she joined VITO as domain responsible for thermal energy systems at EnergyVille, a joint initiative for research in the energy domain in Belgium. Her research interests include, but they are not limited to, numerical and analytical methods for electromagnetic field calculations electrodynamics of deformable materials and integrated design, (numerical) optimization, control and (re) use of energy-efficient, reliable and cost-effective electric/hydraulic drive systems with applications in robotics, e-mobility, and manufacturing industry. Design, analysis and optimization of renewable based multi-carrier energy systems in smart, sustainable systems, including district heating and cooling are among her more recent research activities.